AN ABSTRACT OF THE THESIS OF

Nick West for the degree of Honors Associate Baccalaureate of Science in Bioresource Research presented May 16th, 2014. Title: The Challenge of Finding Where SOD Gets Zinc: Identifying Novel Techniques to Recombinantly Express Metallothionein.

Abstract approved:

_____

Joseph Beckman

Amyotrophic Lateral Sclerosis (ALS) is a neurodegenerative disease where paralysis of the body is the result of motor neuron function loss. A potential cause of ALS is the loss of zinc from Superoxide Dismutase (SOD). SOD's cellular responsibility is to enzymatically react with the superoxide anion forming oxygen and the less hazardous chemical species of hydrogen peroxide. In order for SOD to be stable and fully functional it must be bound to both copper and zinc. When SOD undergoes a variety of mutations, the specifically folded protein is more susceptible to lose the zinc atom. Research has shown the loss of zinc from SOD can activate SOD to create toxic intermediates that can stimulate motor neuron cell programmed death and ALS onset. The source and exact processes by which SOD receives its zinc atom has yet to be fully described. A potential family of proteins responsible for SOD's zinc are the group known as the Metallothionein's.

Metallothionein's are a family of metalloenzymes critical to regulating cellular zinc concentration levels. The combination of low molecular weight and the high amount of cysteine residues makes this protein exceptionally difficult to analyze in vitro and in vivo. Using recombinant DNA experimental techniques the Metallothionein isoform 2 gene was successfully inserted into the pTYB11 plasmid using restriction endonucleases *EcoRI* and *SapI*. Attempted expression of Metallothionein using the expression strain, BL21(DE3) pLysS showed unsuccessful induction of Metallothionein expression. However, utilizing the Shuffle T7 expression system provided some evidence that metallothionein isoform 2 was expressed. Thus, our present results seem to hint at an easier form of expressing Metallothionein in bacterial cells, but inherent flaws in the efficiency of the protein's expression still exist.

Keywords: Amyotrophic Lateral Sclerosis, Metallothionein, Restriction Endonucleases, Protein Expression

Corresponding e-mail address: westni.b@gmail.com

The Challenge of Finding Where SOD Gets Zinc: Identifying Novel Techniques to Recombinantly Express Metallothionein

By Nick West

A PROJECT
submitted to

Oregon State University

University Honors College

In partial fulfillment of
the requirements for the
degree of

Honors Baccalaureate of Science in Bioresource Research (Honors Associate)
Minors: Chemistry, Toxicology
Options: Toxicology, Biotechnology

Presented May 16th, 2014
Commencement June 14th, 2014

Honors Baccalaureate of Science in Bioresource Research project of Nick West presented on May 16th, 2014.

APPROVED:

_____

Mentor Joseph Beckman, representing Biochemistry/Biophysics

_____

Committee Member Daniel Sudakin, representing Toxicology

_____

Committee Member Katharine Field, Director, Department of Bioresource Research

_____

Toni Doolen, Dean, University Honors College

I understand that my project will become part of the permanent collection of Oregon State University Honors College. My signature below authorizes release of my project to any reader upon request.

_____

Nick West, Student, Author

TABLE OF CONTENTS

Page

LIST OF FIGURES

Figure Page

Introduction

Amytrophic Lateral Sclerosis (ALS) is a highly destructive neurodegenerative disease that attacks motor neurons and leaves patients paralyzed and even dead within five years of diagnosis. Commonly known as Lou Gehrig's disease, ALS has proven difficult for researchers to identify the exact disease mechanism and any known cures for it. The focus of our research group is on familial Amyotrophic Lateral Sclerosis (fALS). This has led to the study of the role of metallothioneins. Here we describe the successful cloning and potential expression of metallothionein isoform 2.

In 1993 Rosen *et al.* discovered a tight genetic linkage between the onset of ALS and missense mutations in the gene encoding Superoxide Dismutase 1 (SOD1) [1]. When correctly functioning, SOD1 has copper and zinc bound to it and catalyzes the dismutase reaction of superoxide into the less cytotoxic product of hydrogen peroxide [2]. However, various mutations to the SOD1 gene cause the metalloenzyme to misfold and lose the zinc atom. This loss of the zinc atom has been implicated as a critical step in causing SOD1 to initiate ALS symptoms [3].

In 1997 Culotta *et al* discovered that SOD1 received its copper atom by means of a human copper chaperone for SOD1 (CCS) [4]. This stood as a significant step in understanding the critical posttranslational modifications that SOD1 undergoes. However, little is known about how SOD1 receives its zinc.

Potential transporters of zinc to SOD1 are a family of metalloenzymes known collectively as metallothioneins (MT). More specifically, MT isoform 2 (MT) has been proposed as the best candidate for the source of SOD1's zinc. Research has shown the critical role of MT in the transport of metals and metal buffering capabilities [5].

Superoxide Dismutase

SOD1 is unique to eukaryotic organisms that rely on oxygen as a source of oxidative respiration. The SOD1 enzyme is involved in neutralizing superoxide, a potent free radical generated as a by-product of aerobic metabolism. SOD identifies as a distinguishing evolutionary characteristic of eukaryotes in comparison to anaerobic bacteria [6]. Anaerobic bacteria cannot utilize oxygen as a final electron acceptor and therefore do not express a protein like SOD.

SOD1 Structure

SOD1 is a homodimeric protein where both monomers are bound to a copper and zinc molecule. Over forty years ago the unusually large half-life of Cu,Zn SOD1 was identified [6].

Each SOD1 monomer contains 153 amino acids with each corresponding monomer having 8 β-barrel secondary structure characteristics [3]. The random loops (Figure 1) possess specific properties for the proteins stability, as well. The yellow random loop, known as Loop IV, (Figure 1), participates in interacting favorably with the other monomeric subunit to increase homodimeric stability. This sub-loop of Loop IV creates 38% of the contact area between the two monomers [3]. Certain structural characteristics of SOD help with the physical integrity and protein function. The disulfide bond, C57-C146 forms a key interaction in forming the stable homodimer [7]. The C57-146 disulfide bond, along with other random loop interactions help in keeping the two subunits intact.

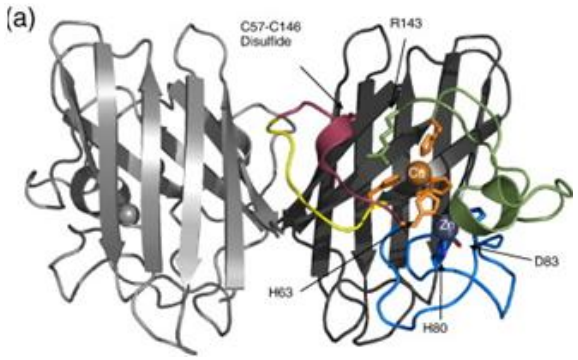

Figure 1. Crystallographic Structure of SOD1: This figure displays the key structural features of SOD1. The C57-C146 disulfide bond acts as a stabilizing bond for the homodimer. Loop IV also acts to stabilize the homodimer, as well as bind to the zinc atom. *Image provided by Blaine Roberts, 2007* [3].

In order to be stable and therefore functional SOD1 must have zinc and copper atoms bound. Zinc and copper must be coordinated via amino acid binding in very specific ways. Any variance in amino acid size or polarity can greatly affect overall protein stability and function.

A section of Loop IV contains the zinc binding residues. The residues that coordinate with zinc are His63, His71, His80, and Asp83 [3]. All four of these amino acid residues contain lone pair electrons that are able to bind with zinc in a detailed fashion. Histidine contains an amine group with a lone pair of electrons that are highly attracted to the positive Zn^{2+} atoms. A similar situation occurs with aspartic acid. This amino acid residue has a carboxylic acid moiety that is attracted to the electropositive zinc atom.

Copper is bound internally relative to the zinc atom. Copper is coordinated by amino acid residues His63, His46, His48, and His120 [3]. Interestingly, the His63 coordinates with both the zinc and copper atoms. The bridging ligand known as His 63 is critical and mutation to this histidine makes protein stability exceptionally vulnerable [3]. This form of a histidine bridging ligand has only been observed in Cu,ZnSOD1 [8]. The important aspect to note is that zinc and copper are bound in a subtle conformation where any change to amino acid residues has a significant chance of directly affecting the binding ability of zinc.

SOD1 Catalytic Function

Superoxide (O_2^-) is a product resulting from the electron transfer chain during mitochondrial aerobic respiration. Free radical containing superoxide is formed when O_2 is incompletely broken down into H_2O [8]. Superoxide can be very damaging to cells and tissues of organisms. Superoxide is particularly damaging to proteins dependent on Fe(II) because the free radical electron on superoxide can change the oxidation state of metals [8]. The body has adapted to this toxic free radical by producing SOD1.

The role of SOD1 is to effectively neutralize the harmful superoxide radical. SOD1 accomplishes this by means of metal ion catalysis using the Cu(II) atom. The superoxide substrate is guided to the active site by means of an electrostatic Loop VII, which attracts or repels the substrate through to the positively charged Cu(II) [3][9]. Lys134 and Glu131 act as key residues in coaxing the substrate to the active site and Arg143 appears to position superoxide for the subsequent reaction [9]. Crystallographic assays have shown SOD1 to have a large 24 Å channel in its conformation that gradually narrows down to a 4 Å opening directly above the copper atom [8]. This ingenious technique to bind to superoxide ensures rapid substrate binding to active site.

Upon binding and orientation the first superoxide radical undergoes oxidation by giving its extra electron to Cu(II), reducing the atom to Cu(I) [8]. As Figure 2 shows, after this initial reaction occurs another superoxide molecule is brought to the active site and reacted with Cu(I) plus two hydrogen protons that result in the formation of hydrogen peroxide [8].

$O_2^- + Cu(II)ZnSOD \rightarrow O_2 + Cu(I)ZnSOD$

$O_2^- + Cu(I)ZnSOD + 2H^+ \rightarrow H_2O_2 + Cu(II)ZnSOD$

Figure 2. Reaction mechanism for SOD1 with Superoxide: In this reaction superoxide reacts with SOD twice to form hydrogen peroxide. *Equation provided by John Hart, 1999* [8].

Amyotrophic Lateral Sclerosis and SOD1

Amyotrophic Lateral Sclerosis represents one of the greatest conundrums of modern medicine. The disease was discovered over 125 years ago by the French scientist Jean-Martin Charcot, yet the exact disease mechanism and its cure still remains elusive for researchers. ALS has a prevalence rate of 3 in 100,000 in the population, but a large increase in risk for individuals over 50 years old does occur [10]. The most common form of ALS randomly occurs in individuals without any apparent genetic causative agent. This is referred to as sporadic ALS and 90-95% of ALS patients have this form of the disease [10]. The other form of ALS has a strong genetic linkage and is known as familial ALS (fALS). Familial ALS is an autosomal dominant disease in which greater than 85% of heterozygous individuals contract the disease [11]. Familial ALS may only account for 5-10% of total ALS disease reports, but a great amount of current research focuses on this area in order to identify a disease mechanism.

Over 20 years ago a group of researchers identified commonality amongst some ALS patients. Studying the DNA of ALS patients they found numerous mutations in the SOD1 gene [1]. Since this breakthrough, over 130 mutations in SOD1 have been shown to induce the ALS disease. Mutated SOD1 comprises 25% of fALS patients and over 2% of all ALS cases [3]. A multitude of theories attempting to describe the mechanism of fALS by way of mutated SOD1

exist. Some of these theories revolve around zinc deficient SOD1 and the resulting toxic gain of function of SOD1 [10].

In the toxic gain of function theory for mutated SOD1 fALS. The idea is that protein stability is based largely on very discrete and specific amino acid residue bonds. Any distortion in charge type or amino acid polarity can significantly alter overall protein function.

Mutant and wild type forms of SOD1 are expressed equally in fALS patients [12]. Certain mutations to SOD1 result in no observable loss in its ability to scavenge the free radical superoxide. However, researchers find that specific mutations to SOD1 that result in a 60% decrease in activity [13]. In some instances mutant SOD1 is able to scavenge superoxide at a fairly similar rate as wild type SOD1 [3]. The vast majority of mutations in SOD1 shown to cause fALS are found outside of the active site pocket. Only two such mutations actually affect the active site. The most common mutation is the missense mutation of the fourth position alanine to a valine (A4V) residue [14].

Inherent flaws in mutant SOD1's stability and ability to hold on to zinc. The mutations in SOD1 indirectly decrease the overall affinity of SOD1 for zinc. Mutant SOD1 has a 5 to 50 fold decrease in affinity for zinc when comparing to wild type SOD1 [15].

A simple, but highly insightful, biochemical assay demonstrated the increased toxicity of zinc deficient Cu-SOD1.When copper is in its neutral form it is green in color. The oxidized form of copper is teal. Adding ascorbic acid to WT Cu,Zn SOD1 and A4V Cu,Zn-SOD1 resulted in no oxidation of copper. In Figure 3 these controls are represented by the two green tubes. However, the addition of ascorbate to A4V zinc deficient SOD1 resulted in a 3000 fold increase in oxidation of copper [15]. In Figure 3 these reactions are shown by the single teal tube. Reduction of ascorbate acid was done by reducing Cu to Cu^{+} through altering the His63 bridging ligand. This test demonstrated the reducing effect of Zn deficient SOD1, but further tests were required to show its relevance to fALS.

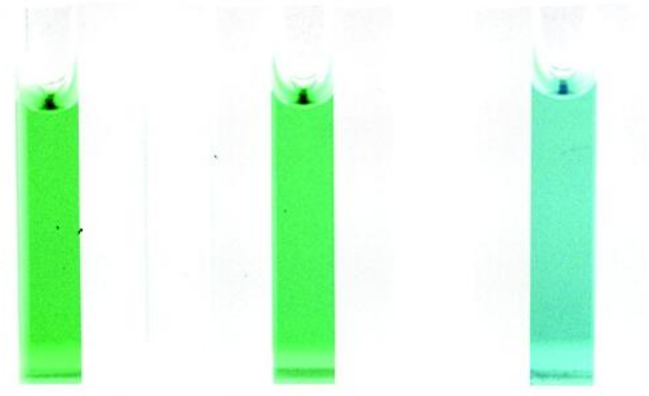

Figure 3. Oxidation of ascorbate by zinc deficient SOD1: Wild Type Cu,Zn SOD1 and A4V Cu,Zn SOD1 plus ascorbate shown in green. A4V Zn deficient SOD plus ascorbate shown in blue. *Image provided by Alvaro Estevez, 1999* [15].

SOD1 Toxic Gain of Function via Zinc Deficiency and Nitric Oxide

Each muscle in the human body is coordinated with a single motor neuron. Nitric oxide is a common biological regulator of plasticity in the cardiovascular and nervous systems [16]. Current theories regarding the biochemical mechanism for the toxic gain of function of SOD1 revolve around the chemistry that occurs between nitric oxide and superoxide and the subsequent interactions with Zn deficient SOD1.

Research has shown that introduction of liposomes containing WT Cu,Zn SOD1 and mutant Cu,Zn SOD1 to cultured motor neuron cells was not toxic [15]. Neither the wild type nor mutant form of copper and zinc containing SOD1 conferred toxicity to the cells. However, the introduction of liposomes containing Zn deficient wild type and mutant form of SOD1 induced motor neuron apoptosis [15]. Copper chelators were also introduced to zinc deficient SOD1 and the motor neurons were subsequently able to survive and grow. The copper chelators were used to pull out the copper from the zinc deficient SOD1 and identify if the presence of copper was necessary to induce apoptosis. As a result of the chelator addition motor neuron apoptosis was saved and the neurons showed no effect. This demonstrated that copper was a critical factor in the induction of motor neuron apoptosis [15].

Nitric oxide synthase (NOS) creates nitric oxide for various cellular systems including motor neurons. *Estevez et al*. demonstrated that introduction of NOS inhibitors rescued Zn-deficient SOD1 motor neuron cells [15]. This finding led researchers to believe that nitric oxide had a fundamental role in the apparent toxic gain of function theory for fALS.

Nitric oxide reacts with superoxide at a rate of 6.7×10^9 $s^{-1}M^{-1}$. Superoxide reacts with nitric oxide three times faster than with wild type SOD1 [16]. The resultant product from the

reaction of nitric oxide and superoxide is the highly oxidizing agent, peroxynitrite ($OONO^-$). Peroxynitrite in turn reacts with SOD1 at a rate of ~10^5 $s^{-1}M^{-1}$ [16]. The resulting product of the SOD1 and peroxynitrite reaction is a nitronium intermediate that is believed to react further with tyrosine amino acid residues. Figure 4 demonstrates the general chemical reaction of the generation of the nitronium intermediate. The nitration of tyrosine residues is believed to set off a cell death cascade. This raises the question of why Zn deficient SOD1 has a toxic gain of function and reacts more preferentially with peroxynitrite and not superoxide.

$$SOD\text{-}Cu^{2+} + ONOO^- \rightarrow SOD\text{-}CuO\ldots.NO_2^+$$

$$SOD\text{-}CuO\text{---}NO_2^+ + H\text{---}Tyr \rightarrow SOD\text{-}Cu^{2+} + HO^- + NO_2\text{-}Tyr$$

Figure 4. Proposed reaction mechanism for the reaction of $OONO^-$ with SOD1. *Equation provided by Joseph Beckman, 1993* [16].

The implications for the Zn-deficient SOD1 theory for fALS disease onset and the reaction with peroxynitrite lie in the structural conformation change in mutant SOD1. For years researchers have theorized that the lack of toxicity of Cu,Zn SOD1 was due to the inability for peroxynitrite to react with the copper group [17]. Furthermore, it has been proposed that only the trans isomer of peroxynitrite would be capable of entering the active site and reacting with copper [17]. Figure 5 demonstrates the proposed mechanism by which peroxynitrite could react with SOD1. In essence, it was thought that the large electronegative peroxynitrite could not fit into the active Zn,Cu-SOD1 active site pocket and eventually form the nitronium intermediate. Therefore, it was believed that the loss of zinc created a conformational shift that exposed the copper atom to more oxidizing agents such as peroxynitrite. Ultimately, the structural

characterization using crystallography of Zn-deficient SOD1 demonstrated a significant conformational change surrounding the copper atom [3].

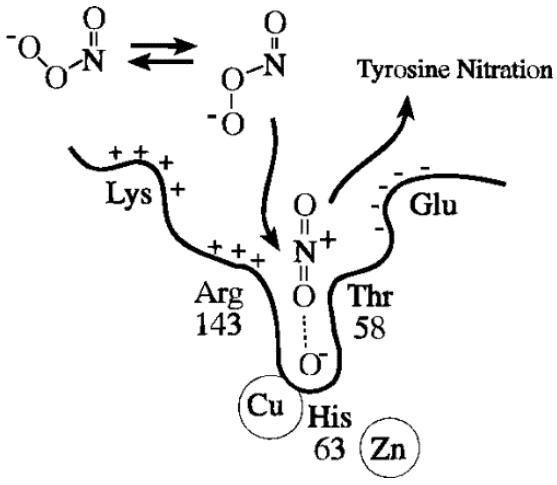

Figure 5. Conformational selectivity of Cu,Zn SOD1 against reacting with peroxynitrite: The narrow opening to the Cu atom is a form of conformational selection in ensuring that oxidative species like peroxynitrite are not allowed into the active site. It is believed that only the trans form of peroxynitrite would be able to react with Cu,Zn-SOD1. *Image provided by Joseph Beckman, 1996* [17].

The Zn-deficient SOD1 crystallography showed the electrostatic loops in disarray. The SOD1's electrostatic loops are essential in the guiding of superoxide to the active copper site. In the Zn-deficient protein the active site is exposed to a greater degree because of the electrostatic loop disorganization and the zinc binding loops demonstrate increased exposure of the copper atom [3]. Figure 6 shows digitized versions of the crystallographic assays, which reveal a narrowing hole in the Cu,Zn-SOD1 (Figure 7a) that goes from 12 Å to 4 Å. However, this narrow tunnel to the copper active site is no longer present in the Zn-deficient display (Figure 6b).

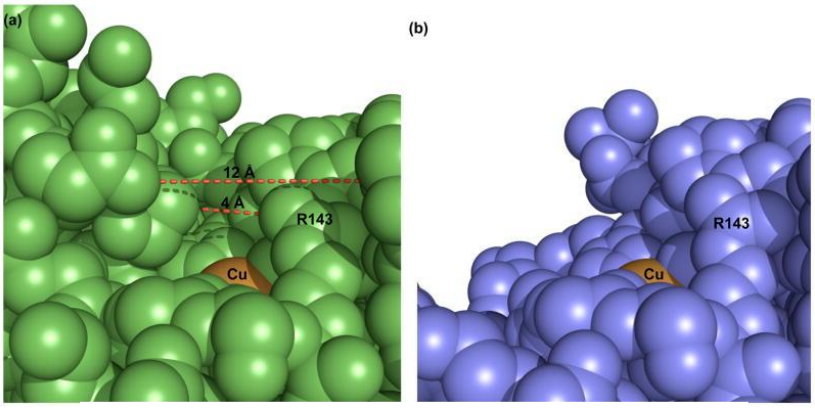

Figure 6. Increased copper accessibility in Zn-deficient SOD1. *Image provided by Blaine Roberts, 2007* [3].

Once it was understood how the Zn-deficient SOD1 was structurally capable of reacting with peroxynitrite the research focus shifted to determining how the resulting nitronium intermediate could cause motor neuron apoptosis.

In 2013 researchers discovered a potential mechanism for cell death in motor neurons in ALS. The critical protein involved in this pathway is the 90 kDa heat shock protein (HSP90). HSP90 is a chaperone protein expressed in all eukaryotic cells and acts as a homeostatic regulator of cellular processes [18]. The normal function of HSP90 involves stabilizing specific proteins during cellular stress. With over 200 client proteins HSP90 has a central role in protecting cells during high heat environments, mechanical stress, and pH imbalances. However, much like Zn-deficient SOD1, nitrated HSP90 displays a similar toxic gain of function.

Researchers discovered that when nitrated tyrosine HSP90 was delivered to motor neurons via the Chariot system cell death occurred [18]. Interestingly, further probing demonstrated the nitration of one specific amino acid was enough to induce apoptosis. Nitration of tyrosine residues Tyr-33 and Tyr-56 in the presence of peroxynitrite created a toxic gain of function for HSP90 [18]. The experimentally designed formation of mutant HSP90 using Y33F

and Y56F did not induce apoptosis in the presence of peroxynitrite [18]. Phenylalanine was used in the mutant forms because this unreactive residue cannot be nitrated. Figure 7 is a crystal structure of HSP90 showing the tyrosine sites prone to nitration. The next task was to identify exactly how nitrated HSP90 resulted in a toxic gain of function and ultimately apoptosis.

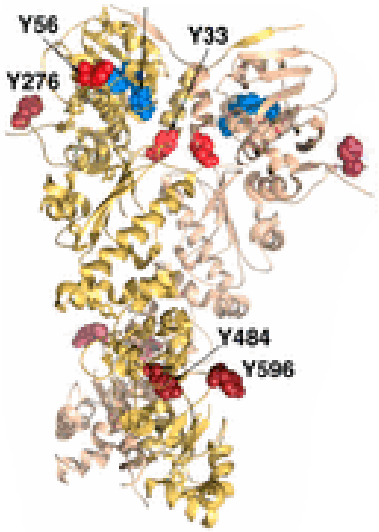

Figure 7. Nitrated HSP90 crystal structure: Diagram of nitrated tyrosine amino acid residues. Residues Y484, Y596, and Y276 did not induce apoptosis when nitrated unlike residues Y33 and Y56. *Image provided by Maria Franco, 2013* [18].

Research has shown that when motor neurons are in low level trophic factor environments the motor neurons undergo programmed cell death [19]. Trophic factors are cellular signaling molecules that signify for cellular growth. One specific mechanism of programmed cell death is via the Fas death receptor cascade. The activation of Fas results in two different cell death pathways.

One pathway involves the activation of Fas-ligand (FasL). FasL in turn causes the release mitochondrial cytochrome *c* [18]. Research has shown that the release of mitochondrial

cytochrome *c* causes a series of reactions that ultimately activates the caspase mediated cell death pathway [20]. Caspases are cysteine proteases that cleave a multitude of proteins and thereby halting cellular function. This cellular signaling cascade can be found in most human cell types.

The other pathway is specific to motor neurons and provides a relevant model for ALS. Raoul *et al.* discovered that mutant SOD1 expressing motor neurons were particularly prone to cell death via Fas caspase 8 pathways [19]. However, further investigation demonstrated it was not the mitochondrial cytochrome *c* pathway, but a novel signal transduction cell death mechanism. In this pathway the activation of Fas and FasL resulted in the eventual activation of nitric oxide synthase (NOS) [21]. The production of nitric oxide results in the ultimate formation of peroxynitrite [16]. As mentioned previously, peroxynitrite has been shown to react with Zn-deficient SOD1 to form a nitronium intermediate capable of nitrating tyrosine residues.

Franco *et al.* discovered that nitrated HSP90 activated the cell receptor P2X7 [18]. Activation of P2X7 allows Ca^{2+} to flow into the motor neuron. The release of calcium initiates the binding of FasL containing vesicles to the cell membrane and induces the Fas cell death cascade via the mitochondrial cytochrome *c* pathway [18].

The creation of nitrated tyrosine residues on HSP90 via mutant SOD1 dependent nitronium intermediates and the subsequent release of calcium by P2X7 results in motor neuron death [18]. The connection between mutant SOD1 and the specific motor neuron cell programmed death creates a unified picture explaining how SOD1 influences and/or causes fALS. Figure 8 illustrates the proposed cellular signaling mechanisms incorporating mutant SOD1, nitrated HSP90, P2X7, and the two Fas pathways.

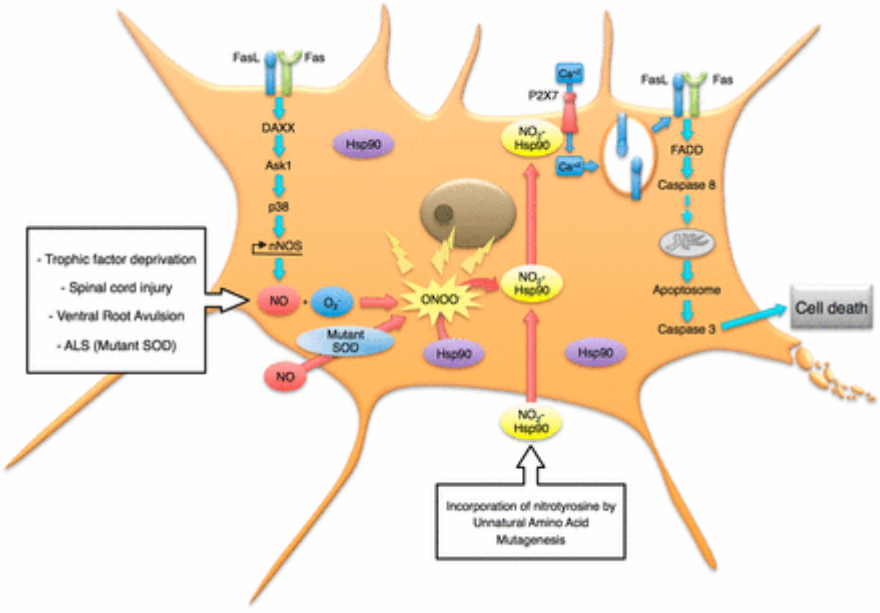

Figure 8. Model for the nitrated HSP90 mediated cell death signaling pathway. *Image provided by Maria Franco, 2013* [18].

Axonal Degeneration and fALS Disease Progression

It has long been observed that some muscular neurodegenerative diseases involve the gradual retraction of distal synapses and axons. These processes can manifest far before any perceived symptoms in the patient or study animal [22]. In diseases like ALS, Huntington's, Parkinson's, and Alzheimer's a common trend of axonal and synaptic degeneration prior to symptom onset does exist[23]. Furthermore, knocking out the proapoptotic gene Bax protects mutant SOD1 motor neuron axons [24].

SOD1 expression in motor neurons is necessary, but not sufficient to induce motor neuron death [23]. Observing pathological processes of disease in mutant mice lines provided key insight into SOD1 mediated fALS.

Breeding lines of SOD1(G93A) mice typically are symptomatic at postnatal day 90-100 (P90-100) and dead by P135±4 [23]. Axons of motor neurons in these mice were lost during P48-50. Interestingly, the only axons that were lost at P48-50 were fast-fatigable motoneurons (FF) [23].

A single muscle fiber is innervated by a motoneuron, which can branch off and innervate several different individual muscle fibers. Therefore, the degeneration of a single FF motoneuron results in the denervation of a single muscle fiber with the possibility of affecting others, too. This connection between motoneurons and individual muscle fibers is displayed in Figure 9.

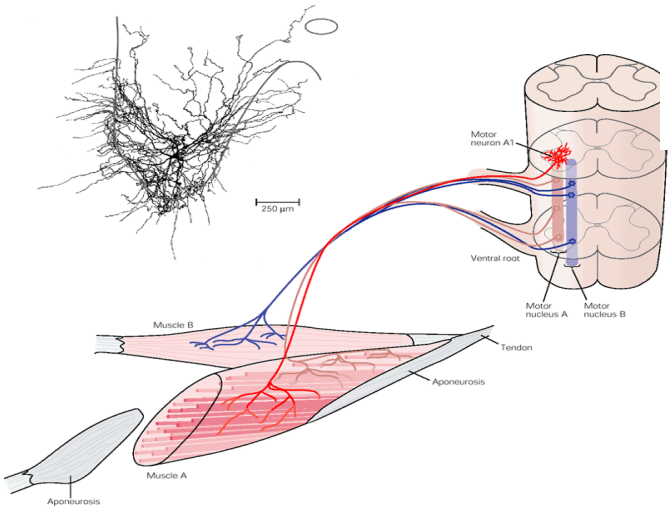

Figure 9. Image of how motoneurons innervate individual muscle fibers. *Image provided by Gerald Loeb* [25]

FF motoneurons are recruited under very specific physiological conditions. FF motoneurons are activated to produce frequent muscular twitches that generate a large amount of force during a short period of time [26]. Whereas slow fatigable motoneurons correspond to slow twitch muscles that generate less force over a much longer (infinite) period of time. Figure 10 compares the fatigability, tetanic force, and twitch display of the three motoneuron types.

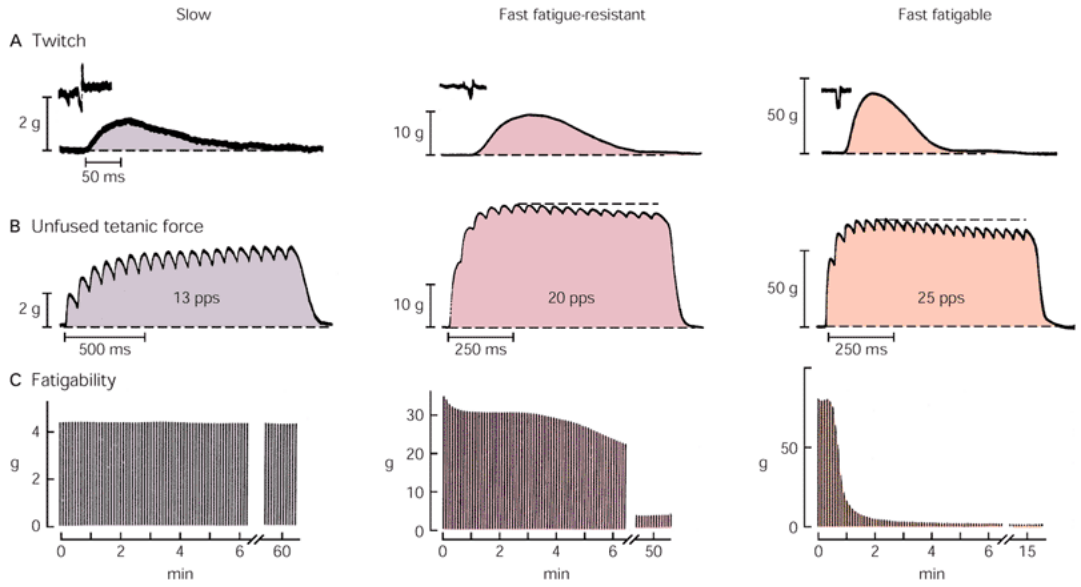

Figure 10. Graphs contrasting muscle types by comparing force to fatigability. Series of graphs depicting differences between slow, fast fatigue-resistant, and fast-fatigable in regards to twitch, unfused tetanic force, and fatigability. *Image provided by Gerald Loeb* [25].

The important finding that SOD1(G93A) mice experience FF motor neuron loss at P48-50 implies that severe motor neuron death occurs for some muscle subtypes while other motor neuron subtypes like slow-fatigable motor neurons remain healthy even after the mice die [23]. By P80-90 all muscle innervation has been destroyed.

Therefore, the muscle is becoming denervated months before the motor neuron is actually dead [27]. Vinsant *et al*. have shown that nervous tissues taken from spinal cord SOD1G93A mice have incredible concentrations of unusual vacuolated mitochondria at P75 [27]. However, motor neurons containing vacuolated mitochondria were also found at the neuromuscular junction (NMJ) at P30 [27]. Figure's 11 and 12 demonstrate ultrastructural analysis comparing the vacuolated mitochondria in the spinal cord at P75 and NMJ at P30.

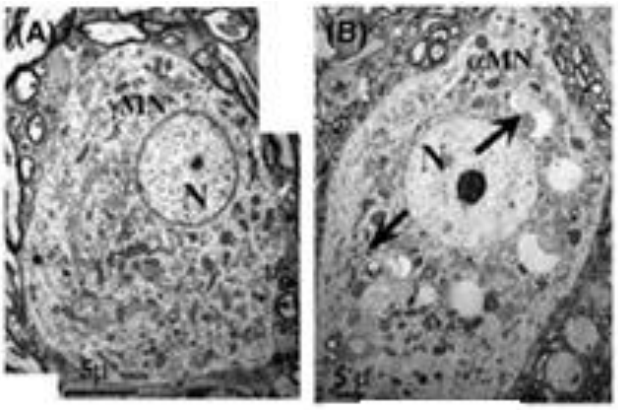

Figure 11. Vacuolated mitochondria at NMJ at P30. Arrows point to vacuolated mitochondria. (A) MN displaying no signs of vacuolated mitochondria. (B) MN displaying vacuolated mitochondria and aggregate vacuoles (C). *Image provided by Sharon Vinsant, 2013* [27].

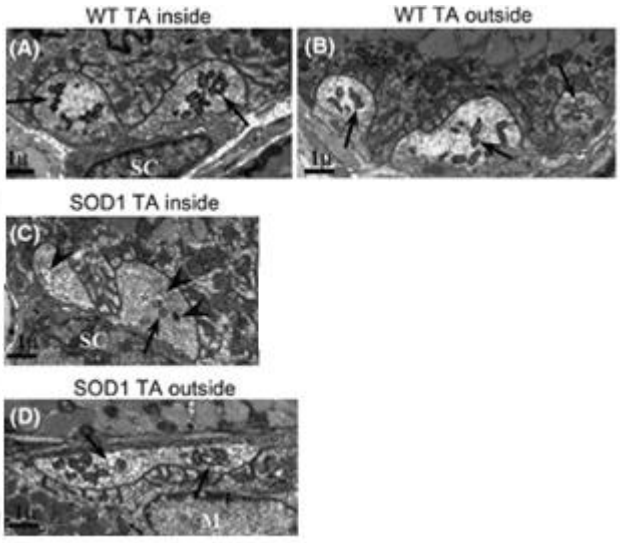

Figure 12. Vacuolated mitochondria in SOD1G93A mice. Arrows point to vacuolated mitochondria. (A) Inside view of WT mouse NMJ at tibialis anterior (TA) muscle with no abnormal mitochondria. (B) Outside view of WT mouse TA NMJ with no abnormal mitochondria vacuoles. (C) Inside view of SOD1 mice TA NMJ at P30 with vacuolated mitochondria. (D) Outside view of SOD1 mice TA NMJ at P30 with vacuolated mitochondria. *Image provided by Sharon Vinsant, 2013* [27].

This demonstrates that damage occurring to the NMJ as early as P30 with denervation occurring at P48-50 followed by spinal cord mitochondrial stress at P75 leads ultimately to MN death at P90-100. This indicates that disease progression is beginning in the distal portions of the peripheral nervous system NMJ and ultimately working its way back to the spinal cord where MN death eventually occurs. Several theories attempt to describe the significance and cause of the vacuolated mitochondria. For example, mitochondrial swelling may be an adaptive response that eventually leads to the release of cytochrome c. [27].

Summarizing ALS Proposed Disease Progression

Overall, it has been established that zinc deficient SOD1 induces motor neuron death. Furthermore, the potential motor neuron cell death mechanism involves zinc deficient SOD1 reacting with peroxynitrite to form a nitronium intermediate that nitrates tyrosine residues on HSP90 ultimately leading to mitochondrial cytochrome c release and caspase mediated cell death. Recent fALS pathology research has identified NMJ vacuolated mitochondria prior to denervation and motor neuron death in $SOD1^{G93A}$ mice [27]. Whether or not the specific mechanisms found by *Franco et al.* are directly causing the pathology described by *Vinsant et al.* is still to be determined.

Metallothionein: The Metal Binding Protein Family

The family of metal binding proteins known as Metallothionein (MT) represents one of the more enigmatic group of proteins in biology. In 1957, Margoshes and Vallee discovered a peculiar protein in equine kidney that was capable of binding cadmium [28]. Four years later Vallee and Kägi identified this protein as MT and noted its ability to bind both cadmium and zinc [29]. For years researchers believed that MT was essential in anti-oxidant activity. However, Maret and Vallee in 1998 postulated the novel function of MT in distributing zinc according to the energy needs of the cell [30].

Metallothionein Isoforms

The genes encoding MT proteins are found on chromosome 16. The family of MT proteins can be divided into major and minor groups based on differences in molecular weight, metal binding, and gene coding. MT isoforms one and two (MT1 and MT2) represent the major groups. MT isoforms three and four (MT3 and MT4) are referred to as the minor groups [31]. The major groups typically bind divalent cations and are expressed in most all tissues while the minor groups are found in specialized cells like the brain and stratified epithelial tissue [32]. MT1 and MT2 expression has been demonstrated in transgenic fALS SOD1 mice [33].

Structural Characterization of Metallothionein

MT has an unusual concentration of cysteine amino acids. Out of the 61 amino acids that comprise the primary sequence of MT, 20 are cysteine's with a total molecular weight of 7 kDa. No aromatic amino acids and no histidine residues in MT are present in the amino acid sequence [32].

Analyzing the primary sequence of MT2 (Figure 13) provides some insight into patterns that occur in the protein. The yellow highlighted boxes represent cysteine residues. A regular pattern noticeable in the sequence is the occurrence of Cys-Xaa-Cys, Cys-Xaa-Yaa-Cys, Cys-Xaa-Yaa-Zaa-Cys, and Cys-Cys motifs. In this case Xaa, Yaa, and Zaa represent amino acids that are not cysteine [32]. This placement of cysteine residues provides an inherent structure for binding metal cations. Another interesting aspect of the primary sequence is the placement of two lysine residues (K-K) directly next to each other. Certain proteases are able to identify this specific motif and subsequently cleave the protein.

gac D	tcc S	tgc C	acc T	tgt C	gcc A	ggc G	tct S	tgc C	aaa K
tgt C	aaa K	gaa E	tgc C	aaa K	tgt C	act T	agt S	tgc C	aag K
aaa K	agc S	tgc C	tgt C	tcc S	tgc C	tgt C	ccg P	gtg V	ggc G
tgc C	gca A	aaa K	tgt C	gca A	cga Q	ggc G	tgc C	atc I	tgt C
aaa K	ggc G	gct A	agc S	gac D	aag K	tgc C	agc S	tgt C	tgc C
gct A	tga Stop								

Figure 13. Metallothionein isoform 2 primary sequence showing the DNA and resulting amino acid sequences. *Data obtained from Bert Vallee, 1960* [29].

Binding of Zinc Atoms by Metallothionein

Metalloproteins, like MT, undergo metal binding posttranslational modifications that require the coordination of specific amino acid residues with a metal (in this case Zn^{2+}) cation. The apo form, thionein, has no known tertiary structure [5]. Typically zinc cations coordinate with four amino acids consisting of either histidine, aspartic acid, glutamic acid, cysteine [34].

MT has two domains, α and β, that can bind 3 and 4 zinc cations, respectively [34]. Figure 14 shows the specific cysteine residues that coordinate with the zinc cations in the two domains. The precise structure of the protein is dependent not only upon what metal is bound, but the number of metals bound to the protein and their locations [34]. The specific zinc binding locations have different affinities for binding the zinc cations. MT2 has four sites that have a high affinity of $K=10^{11.8}$ whereas two intermediate binding sites have an affinity of $K=10^{10}$. The lowest binding site has an affinity of $K=10^{7.7}$ [5]. The different affinities of the different sites implies that MT can regulate zinc levels at varying concentrations.

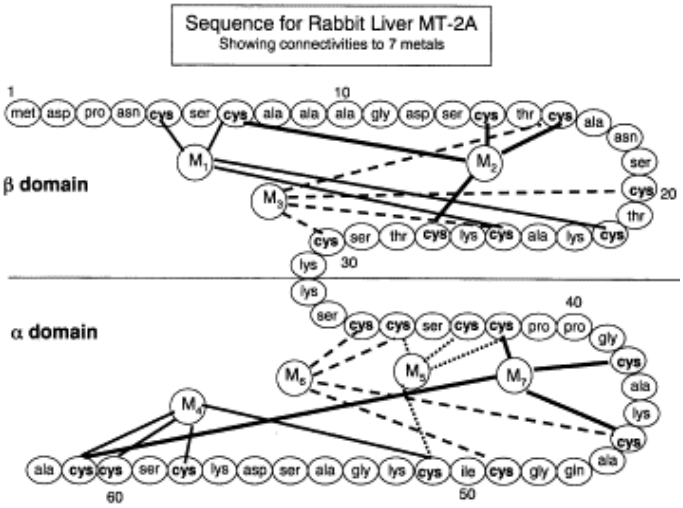

Figure 14. Diagram representing the specific cysteine residues coordinated with divalent metal cations. *Image provided by Jayna Chan, 2002* [34].

Redox Role of Metallothionein

The physiological role of MT's remain relatively unknown. Maret *et al.* provided groundbreaking evidence demonstrating the redox buffering role of MT [5]. The redox buffering capacity of MT's demonstrate the critical monitoring of physiological zinc levels.

The thiol groups in MT correspond to a reduction potential of -366 mV [5]. This very low reduction potential correlates to a high likelihood of oxidation. MT is oxidized in the presence of glutathione disulfide (GSSG) and the zinc atom is subsequently lost [30]. Furthermore, the presence of reduced glutathione (GSH) and GSSG results in the enhanced release of zinc to an apoenzyme [30]. Maret and Vallee performed a simple test in vitro to demonstrate this phenomenon [30]. Figure 15 demonstrates the increased release of zinc in the presence of GSSG and GSH.

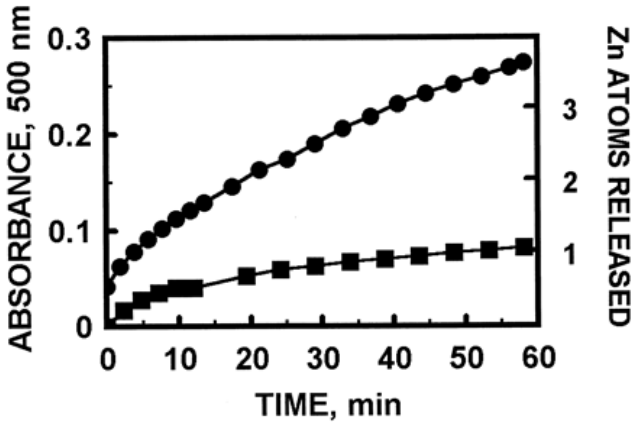

Figure 15. Comparing zinc atoms released to presence or absence of GSH. This graph demonstrates the kinetics of zinc release in MT2. MT2 was incubated in the following conditions: MT2(1.3 uM), PAR(100 uM), Tris-Cl(0.2 M) at pH=7. The block shapes represent the control where GSH is absent. The circle shapes represent the addition of GSH (1.5 mM) and GSSG (3 mM). Absorbance was monitored at 500 nm. *Image provided by Wolfgang Maret, 1998* [30].

The way in which MT transforms from binding zinc to providing zinc to apoenzymes is summarized in Figure 16. This diagram illustrates how zinc bound MT encounters an oxidant (GSSG/GSH, DsbA, etc) and is subsequently oxidized forming a disulfide bond [5]. This form of

the protein is called Thionin. The released zinc atom is thought to be given off to an apoenzyme. The Thionin form is then reduced and becomes the negative Thionein conformation. This Thionein conformation can then react with zinc and reform the MT conformation [5]. Therefore, a plausible zinc cycle was proposed where MT acts as the critical regulatory point in providing or accepting zinc atoms to other metalloenzymes.

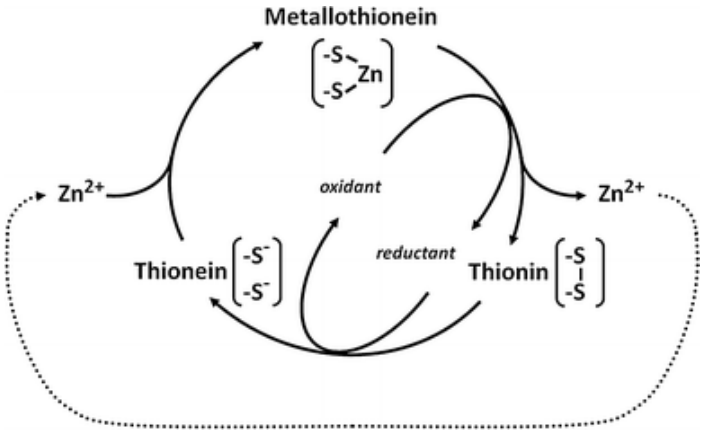

Figure 16. Diagram demonstrating the cyclic redox reaction transforming MT through oxidation into Thionin and eventually binding with zinc again to form MT. *Image provided by Wolfgang Maret, 2011* [5].

Metallothionein's Relevance to SOD1

Zinc forms an integral part in the function of over 3,000 proteins in the human body [35]. Maret has proposed the idea that MT performs the critical function of monitoring zinc concentrations in the cell and providing zinc to proteins that require this metal to be bound in order to be activated [5].

Therefore, the potential for MT to be the source of zinc for proteins like SOD1 remains a topic of interest. SOD1 must have zinc bound in order to perform its normal physiological function. The possibility that SOD1 receives its zinc molecule either directly or indirectly from

MT has yet to be confirmed. Regardless of how SOD1 receives its zinc atom, MT clearly plays a significant role in free zinc concentration levels [5].

However, the low molecular weight paired with the high cysteine residue concentration of MT makes it exceptionally hard to acquire purified MT. The objective of this research, therefore, is to identify a technique to express MT using bacterial *E. coli* cells.

Materials and Methods

MTpUC57 and pTYB11 Digests

GenScript synthesized the MT gene in the plasmid pUC57. The entire sequence coding for MT is 183 base pairs in length. Specific restriction sites were utilized to insert the MT gene into the pTYB11 plasmid. The restriction sites coding for the corresponding endonucleases were *SapI* and *EcoRI*. *SapI* and *EcoRI* restriction endonucleases were applied to both the MTpUC57 plasmid and the pTYB11 plasmid. 900 ng of MTpUC 57 was digested with *SapI* and *EcoRI* according to manufacturer's guidelines. 1 ug of pTYB11 was digested with *SapI* and *EcoRI* according to manufacturer's guideines.

1% agarose gel was used to separate the digested DNA from MTpUC57 and pTYB11. The ~200 base pair band in the MTpUC57 believed to be the MT gene was cut from the gel and purified via a Quiagen Spin Miniprep kit. The digested pTYB11 plasmid was also cut from the agarose gel and purified via a Quiagen Spin Miniprep kit.

Indirect Verification of MT Ligation Into pTYB11

The next step was to insert the MT gene into the pTYB11 plasmid via ligation. DNA ligase was used to insert the MT gene cut from the MTpUC57 plasmid into pTYB11 at the *SapI* and *EcoRI* restriction sites. 90 ng of the pTYB11 vector were used to ligate 100 ng of the MT insert using T4 DNA ligase. Manufacturer guidelines were used for the ligation conditions.

After the ligation had incubated overnight, 4 uL of the MT+pTYB11 (referred hereafter as MTpTYB11) was transferred to a vial of One Shot® TOP10 Competent Cells (Life Technologies). The cells were then plated onto selection Lysogeny Broth (LB) agar plates and incubated overnight at 37°C. The selection plates contained 100 ug/mL of ampicillin.

After the selection plates had incubated overnight a single colony of bacteria was selected and inoculated into 5 mL of LB containing 100 ug/mL ampicillin. This was incubated with shaking for 7 hours at 37°C. The MTpTYB11 DNA was purified from the grow up by a Qiagen Spin Miniprep kit.

The seven digest conditions were20 uL in volume, used Fermentas Digest Buffer (2 uL), and were incubated for 1 hour at 37°C. Digests were ran on the MTpTYB11 plasmid and the empty vector pTYB11 plasmid. Both the MTpTYB11 plasmid and the empty vector pTYB11 plasmid were digested with *NcoI*, *SalI*, and *EcoRI* according to the manufacturer's directions, and resulting fragments were separated on 1% agarose gels."

The results from the seven digests on either MTpTYB11 or pTYB11 were analyzed by 1% agarose gel.

DNA Sequencing

The Center for Genome Research and Bioinformatics at OSU sequenced the MTpTYB11 plasmid using the Sanger Sequencing ABI 3730 capillary sequencing machine.

MTpTYB11 Expression via BL21(DE3) pLysS Competent Cells

The MTpTYB11 plasmid was transferred into *E. coli* BL21(DE3) pLysS competent cells. The cells were cultured overnight at 37°C in 10 mL LB media containing 100 ug/mL ampicillin and 34 ug/mL chloramphenicol. The cultured cells were then transferred to 400 mL LB media.

These cells were cultured at 37°C until the OD_{600} was ~1. IPTG was then added to a final concentration of 0.5 mM and the cells were cultured overnight for 20 hours at 20°C.

Cells were harvested in eight 50 mL centrifugation tubes at 4°C and frozen overnight at -80°C. Ice-cold buffer (20 mM Tris-Cl, pH 7.4, 0.5 M NaCl, 1mM EDTA, 30 mL) was added to each of the eight centrifugation tubes [36]. The thawing action allowed the T7 lysozyme to move out of the bacterial cytoplasm and into the extracellular space. Once outside the cell this lysozyme degrades the *E. coli* peptidoglycan by cutting the amide bond between N-acetylmuramic acid and L-alanine (37), resulting in cell lysis. Pellet and supernatant were collected by centrifugation at 4000 rpm for 10 minutes. Pellets were resuspended in 30 mL of the same ice-cold buffer.

Expression of the intein-MT protein in BL21(DE3) pLysS was checked by 10% SDS-PAGE developed by coomassie stain.

MTpTYB11 Expression via Shuffle T7

The MTpTYB11 plasmid was transferred into *E. coli* Shuffle T7 competent cells. The cells were cultured overnight at 37°C in 5 mL LB media containing 100 ug/mL ampicillin. The cultured cells were then transferred to 200 mL LB media. These cells were cultured at 37°C until the OD_{600} was ~1. IPTG was then added to a final concentration of 0.5 mM and the cells were cultured overnight for 20 hours at 20°C.

Cells were harvested in eight 50 mL centrifugation tubes at 4°C and frozen overnight at -80°C. Ice-cold buffer (20 mM Tris-Cl, pH 7.4, 0.5 M NaCl, 1mM EDTA, 30 mL) was added to each of the eight centrifugation tubes [36]. The samples were sonicated at 4°C (Sonication and

Materials Inc., output control 60, Danbury, CT). The cells were sonicated for 15 seconds and repeated four times. The lysed cells were centrifuged at 4000 rpm for 10 minutes and the resulting supernatant and pellet were collected. The pellet was resuspended with 30 mL of the same ice-cold buffer.

Expression of the intein-MT protein in Shuffle T7 cells was checked by 15% SDS-PAGE developed by coomassie stain.

Shuffle T7 Expression Western Blot

The Shuffle T7 Expression of MT was analyzed by a Li-Cor Western Blot technique. The samples were ran on a 12% SDS gel at 150 volts for 60 minutes. The samples on the SDS gel were then transferred to PVDF paper via electroblotting at 100 volts for 60 minutes. The membrane was then immersed in a blocking solution consisting of 10% powdered milk in Tris buffered Saline (TBS) containing 0.05% Tween-20 for 30 minutes at room temperature. The blot was then incubated with the mouse anti – MT antibody at a 1:1000 dilution. The membrane was then washed with the TTBS buffer solution 3 X 10 minutes with 50 ml/membrane. The membrane was then immersed in TTBS buffer solution with Li-Cor Odyssey 680 nm IRDye at a 1:5000 dilution for one hour. The membrane was then washed with TTBS buffer solution 3 X 10 minutes with 50 ml/membrane. The blotted membrane was analyzed using a Li-Cor Odyssey Scanner.

Results

MTpUC57 and pTYB11 Digests

Figure 17 shows the digests of MTpUC57 and pTYB11 using *EcoRI* and *SapI* restriction endonucleases. In Lane 2 there appeared 3 bands where there should have only been the pUC57 and MT gene bands. A second gene encoding for the *EcoRI* restriction site was found in another part of the pUC57 plasmid. The band in Lane 2 corresponding to ~240 base pairs (bp) was believed to contain the MT gene while the ~208 bp band was believed to have been produced by the errant second *EcoRI* site.

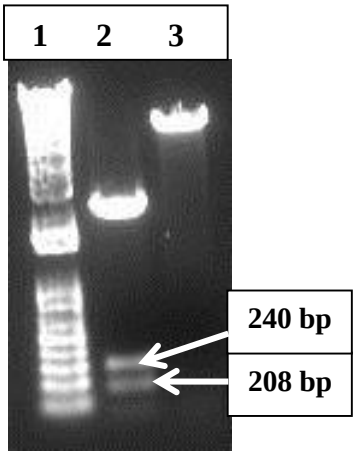

Figure 17. Electrophoresis gel of digested MTpUC57 and pTYB11. 1% agarose gel. Lane 1: 1kB (+) Ladder, Lane 2: MT in pUC57, Lane 3: pTYB11. The MTpUC57 and pTYB11plasmids were digested with *EcoRI* and *SapI*.

Indirect Verification of MT Ligation Into pTYB11

The putative MT gene was inserted into the pTYB11 vector. Indirect verification that the MT gene had correctly been inserted was accomplished by restricting the MTpTYB11 plasmid with *NcoI*, *EcoRI*, and *SalI*. Figure 18 shows the results from these series of digests. The figure depicts 2 agarose gels; one was done in September of 2012 and the other in November of 2013. This was done to insure the digests were replicable.

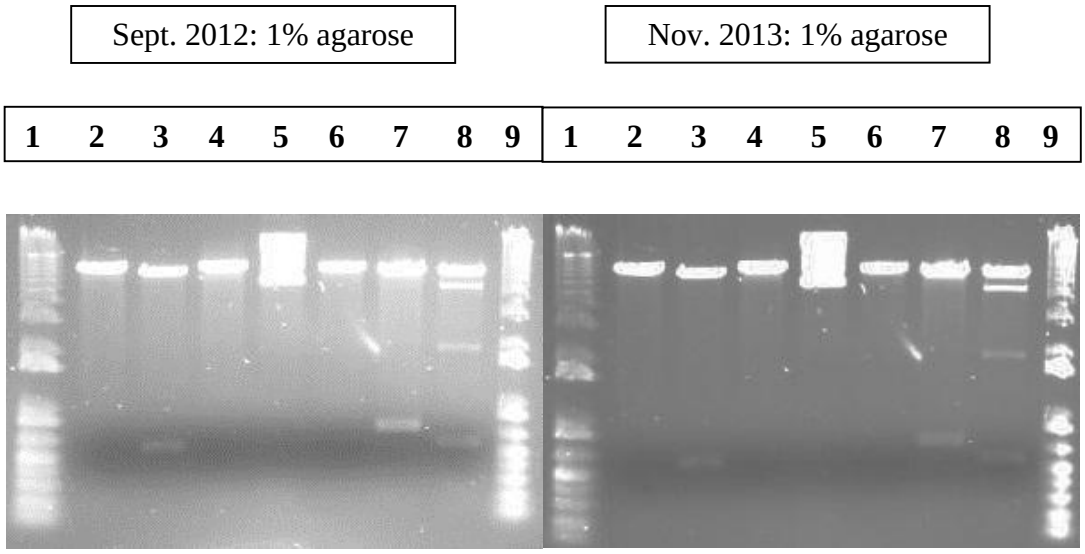

Figure 18. Electrophoresis gels demonstrating the indirect verification that the MT gene had been inserted into pTYB11. 1% Agarose gel with digests using *SalI*, *EcoRI*, *NcoI* restriction enzymes. Lane 1: 1kB plus DNA Ladder, Lane 2: *SalI*/*NcoI* and MTpTYB11, Lane 3: *SalI*/*NcoI* and pTYB11, Lane 4: *NcoI* and MTpTYB11, Lane 5: *SalI* and MTpTYB11, Lane 6: *SalI* and pTYB11, Lane 7: *NcoI*/*EcoRI* and MTpTYB11, Lane 8: *NcoI*/*EcoRI* and pTYB11, Lane 9: 1 kB plus DNA Ladder.

Explanation of the Series of Indirect Digests

Figure 20 displays the series of digests on MTpTYB11 and pTYB11. An explanation of why each digest was done will provide a greater depth of understanding the logic in determining if MT was inserted into pTYB11

Lane 2 Digest: *SalI*/*NcoI* with MTpTYB11

In the pTYB11 plasmid the *SalI* restriction site is located between *EcoRI* and *SapI*. If the segment of DNA sequence between *EcoRI* and *SapI* had been correctly excised by their respective endonucleases the *SalI* restriction site would be effectively destroyed. If the segment

between *EcoRI* and *SapI* had not been excised then the *SapI* to *NcoI* segment would be 568 base pairs in size. However, as seen in Lane 2, the MTpTYB11 digest with *SalI*/*NcoI* procured no bands in the 568 range. In fact the digest of MTpTYB11 resulted in zero bands, except for that which corresponds to the size of the MTpTYB11 plasmid.

Lane 3 Digest: *SalI*/*NcoI* with pTYB11

As mentioned in the explanation of the Lane 2 digest, the *SalI* site is between *SapI* and *EcoRI* restriction sites. The Lane 3 Digest was conducted as a control to demonstrate what would have occurred if the *SalI* restriction site had been present in the MTpTYB11 digest conducted in Lane 2. The Lane 3 digest shows a band at around 600 base pairs. This corresponds to the base pair distance between *SalI* and *NcoI* in the regular pTYB11 plasmid. This shows that the *SalI* restriction site was effectively destroyed in the MTpTYB11 plasmid in Lane 2 and that the *SalI* restriction enzyme was working.

Lane 2 and 3 Digests were placed next to each other to easily reference if the two digests yielded the same or different results.

Lane 4 Digest: *NcoI* with MTpTYB11

The purpose of this digest was to determine if the *NcoI* restriction endonuclease was working. If *NcoI* was not working there would be a smear of DNA observed in Lane 4. The smear would represent DNA in its relaxed and supercoiled form. If *NcoI* was working it would cut the DNA and the plasmid would become supercoiled. The resulting supercoiled band would be a defined band at the 7,000 base pair length. As shown in Figure 17: Lane 4, a defined band demonstrating the *NcoI* enzyme was correctly functioning is observable. This digest was pertinent especially to the digests in Lanes 2 and 3.

Lane 5 Digest: *SalI* MTpTYB11

The purpose of this digest was another technique to determine if the *SalI* restriction site was present in the MTpTYB11 plasmid. If MT had not been inserted into pTYB11 then *SalI* would have cut the DNA at the corresponding restriction site and the resulting band would have been defined and clear. If MT had correctly been inserted into pTYB11 then *SalI* would have had no place to cut the DNA and the resulting band in the gel would be smeared. Lane 5 depicts a smear of DNA in its supercoiled and relaxed forms.

Lane 6 Digest: *SalI* with pTYB11

The purpose of this digest was to act as a control for the digest in Lane 5. *SalI* digested normal pTYB11. The resulting band in Lane 6 was a defined band demonstrating the DNA had been cut at the *SalI* site and was in its supercoiled form.

Lane 5 and 6 Digests were ran next to each other to visually depict the differences between the MTpTYB11 plasmid and the control pTYB11 plasmid.

Lane 7 Digest: *NcoI*/*EcoRI* with MTpTYB11

The purpose of this digest was to determine if MT had been inserted into pTYB11 using the restriction endonucleases *NcoI* and *EcoRI*. If MT had not been inserted into pTYB11 the resulting band for this digest run at 583 base pairs. If MT had been correctly inserted into pTYB11 the resulting band for the digest would run at 766 base pairs. As mentioned before, the MT gene is 183 base pairs in length. Figure 2 Lane 7 depicts a band at 750-800 base pairs.

Lane 8 Digest: *NcoI*/*EcoRI* with pTYB11

This digest acted as a control to the digest in Lane 7. *NcoI* and *EcoRI* enzymes reacted with normal pTYB11 to demonstrate what the resulting band would look like if there was not the MT gene present between *EcoRI* and *NcoI*. The resulting band in Lane 8 is just below 600 base pairs which corresponds to the calculated base pairs that should be present if MT had not been inserted.

DNA Sequencing

Results from the DNA sequencing of the MTpTYB11 plasmid are shown in Figures 19 and 20. Figure 19 provides evidence that the pTYB11 sequence is intact and Figure 20 demonstrates that the MT gene was inserted is indeed present in the pTYB11 plasmid.

ggcttagtag tctcggttaa cgcagaacct gctaaggttg acatgaatgt caccaaacat aaaattagtt
ggcttagtag tctcggttaa cgcagaacct gctaaggttg acatgaatgt caccaaacat aaaattagtt

atgctattta tatgtctggt ggagatgttt tgcttaacgt tctttcgaag tgtgccggct ctaaaaaatt
atgctattta tatgtctggt ggagatgttt tgcttaacgt tctttcgaag tgtgccggct ctaaaaaatt

caggcctgct cccgccgctg cttttgcacg tgagtgccgc ggattttatt tcgagttaca agaattgaag
caggcctgct cccgccgctg cttttgcacg tgagtgccgc ggattttatt tcgagttaca agaattgaag

gaagacgatt attatgggat tactttatct gatgattctg atcatcagtt tttgcttgga tcccaggttg
gaagacgatt attatgggat tactttatct gatgattctg atcatcagtt tttgcttgga tcccaggttg

ttgtacagaa c [MT sequence begins here]
ttgtacagaa c [MT sequence begins here]

Figure 19. CGRB Sequencing comparing pTYB11 DNA to sequenced DNA. This figure compares the CGRB DNA sequence to the real DNA sequence of the pTYB11 plasmid directly before the insertion point of the MT gene. Blue letters indicate the pTYB11 sequence and black letters indicate the CGRB sequence.

atggatccga actgcagctg tgcagctggt gactcctgca cctgtgccgg ctcttgcaaa
atggatccga actgcagctg tgcagctggt gactcctgca cctgtgccgg ctcttgcaaa

tgtaaagaat gcaaatgtac tagttgcaag aaaagctgct gttcctgctg tccggtgggc
tgtaaagaat gcaaatgtac tagttgcaag aaaagctgct gttcctgctg tccggtgggc

tgcgcaaaat gtgcacgagg ctgcatctgt aaaggcgcta gcgacaagtg cagctgttgc
tgcgcaaaat gtgcacgagg ctgcatctgt aaaggcgcta gcgacaagtg cagctgttgc

gcttga
gcttga

Figure 20. This figure compares the CGRB DNA sequence to the real DNA sequence of the MT gene. Red letters indicate the pTYB11 sequence and black letters indicate the CGRB sequence.

MTpTYB11 Expression via BL21(DE3) pLysS Competent Cells

The MTpTYB11 plasmid was transformed into BL21(DE3) pLysS competent cells and induced using IPTG. After harvesting the cells the resulting supernatant and pellet were separated on a 10% SDS gel. Figure 21 shows the results of this induction of protein expression. The intein protein should run on a SDS gel at around 63 kDa. However, Figure 21 demonstrates no observable band in this range.

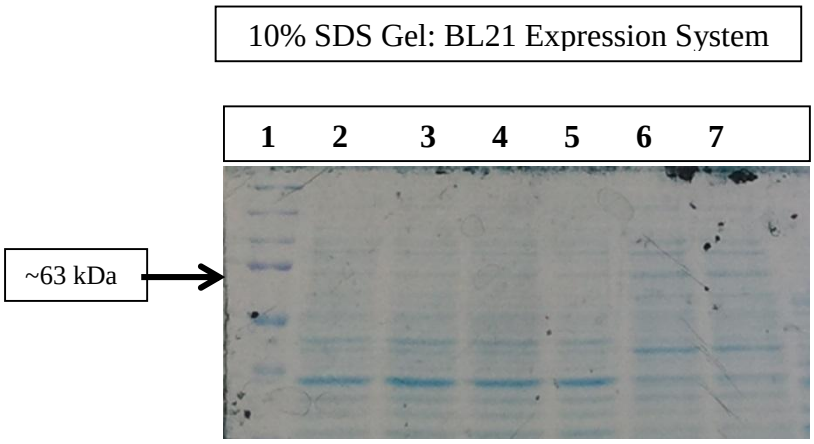

Figure 21. SDS gel of BL21 Expression of MT in pTYB11. 10% SDS gel ran at 150V for 1 hour. Lane 1: Dual Color Protein Standard, Lane 2: Induced MTpTYB11 supernatant, Lane 3: Non-induced sup., Lane 4: Induced pellet, Lane 5: Non-induced pellet, Lane 6: Dual Color Protein Standard.

MTpTYB11 Expression via Shuffle T7

The transformation and induction of Shuffle T7 cells containing MTpTYB11 was analyzed by 12% SDS gel. Figure 22 shows the results. The bands at 63 kDa provide a strong indication that the intein protein was correctly expressed. The amount of protein (in ug) was calibrated with the Bradford Assay.

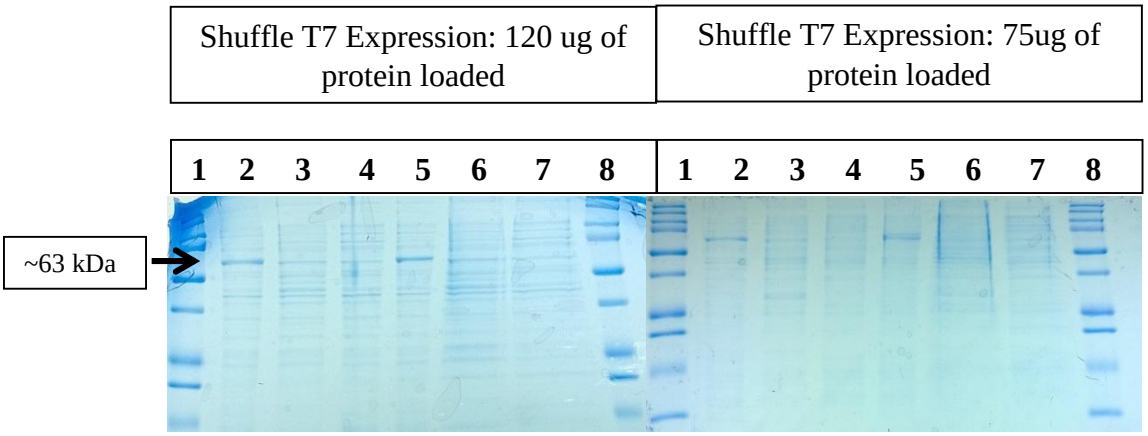

Figure 22. SDS gel of Shuffle T7 expression of MT in pTYB11. Both gels are 12% SDS and were ran at 150V for 1 hour. The lanes of the two gels match up in their contents. Lane 1: Dual Color Protein Standard, Lane 2: Induced MTpTYB11 supernatant, Lane 3: Non-induced MTpTYB11 sup., Lane 4: Empty Shuffle T7 sup., Lane 5: Induced MTpTYB11 pellet, Lane 6: Non-induced MTpTYB11 pellet, Lane 7: Empty Shuffle T7 pellet, Lane 8: Dual Color Protein Standard.

Shuffle T7 Expression Western Blot

To identify if MT had been expressed a Western Blot analysis was done by Li-Cor Odyssey Scanner. Figure 23 is the image produced from the Li-Cor Odyssey Scanner. Evidence showing MT not present in the Shuffle T7 samples is indicated by no significant bands were present in the Shuffle T7 expression (Lanes 2-3, and 5-7). Indiscriminate banding at high molecular weights and vague banding at low molecular weight in the homogenized mouse liver positive control demonstrates a lack of consistency in the MT antibody activity.

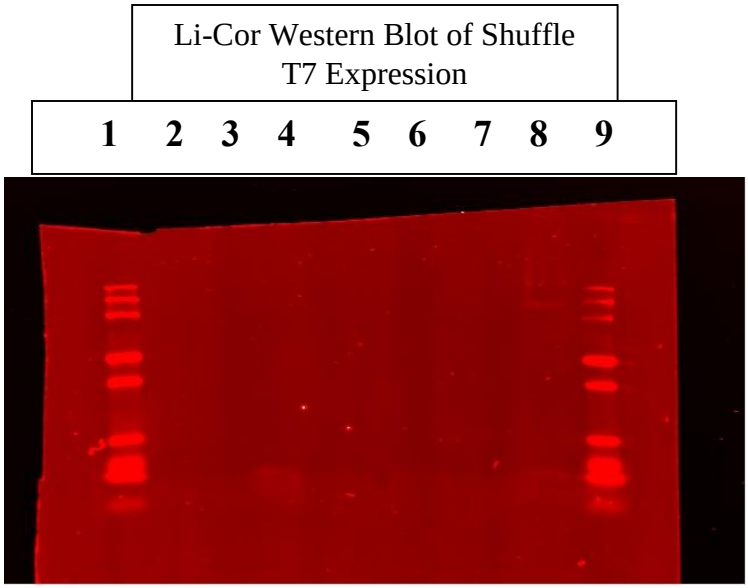

Figure 23. Li-Cor Western Blot of Shuffle T7 Expression. Lane 1: Dual Color Protein Standard. Lane 2: Induced MTpTYB11 Shuffle T7 supernatant. Lane 3: Non-induced MTpTYB11 Shuffle T7 supernatant. Lane 4: Homogenized mouse liver. Lane 5: Induced MTpTYB11 Shuffle T7 pellet. Lane 6: Non-induced MTpTYB11 Shuffle T7 pellet. Lane 7: Empty Shuffle T7 pellet. Lane 8: Homogenized mouse liver. Lane 9: Dual Color Protein Standard.

Discussion

Critical Indirect Verification of MT Insertion

Initial results indicated the MT gene had correctly inserted into the pTYB11 plasmid. Further controls and digests were necessary to conclusively determine the MT gene had been inserted.

Figure 24 represents an overview of regions of the pTYB11 plasmid, as well as certain restriction sites within the DNA sequence. The red region is the multiple cloning site MCS. The yellow section is the chitin binding domain sequence. MT was inserted using *EcoRI* and *SapI* restriction enzymes. The grey and black arrows in Figure 24 represent these sites on the plasmid respectively.

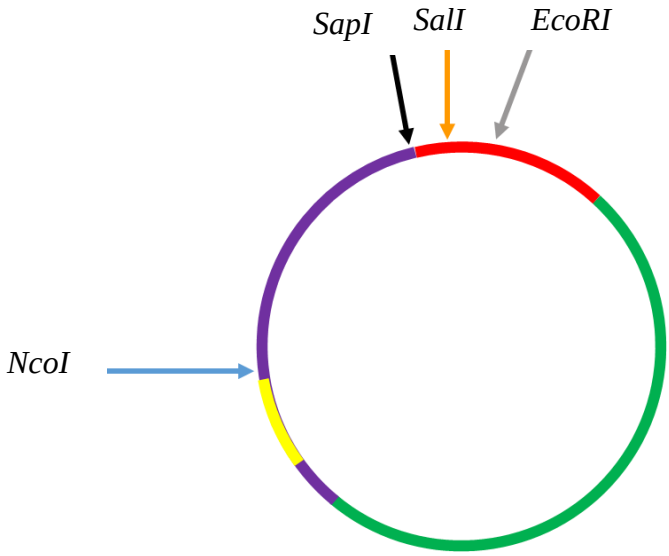

Figure 24. Diagram outlining the intein and multiple cloning regions of pTYB11 along with pertinent restriction sites. The purple region encodes for the intein protein

The orange arrow represents the *SalI* restriction site. The use of the *SalI* restriction enzyme was useful in proving that the segment between *SapI* and *EcoRI* had been excised because the *SalI* site is between those two sites. The blue arrow represents the *NcoI* restriction site. *NcoI* was useful because it was several hundred base pairs away from where MT was ostensibly inserted and could provide insight into whether or not the gene had been inserted.

Using *EcoRI*, *SalI*, and *NcoI* a series of digests were set up to determine if MT had indeed been inserted into pTYB11.

The digests using *EcoRI*, *SalI*, and *NcoI* were critical in indirectly confirming that MT had been correctly inserted into the pTYB11 plasmid. If the MT gene had not been inserted into the pTYB11 plasmid then expression of the MT protein would have been impossible and further expression attempts would have been futile.

Furthermore, the CGRB DNA Sequence conclusively determined that the MT gene had not only been inserted into the pTYB11 plasmid, but that it had been inserted into the correct position in the DNA. If the MT sequence had been inserted out of the open reading frame (ORF) then correct gene expression would have been incapable of producing MT and intein proteins.

Comparing Shuffle T7 and BL21 Expression of MT/Intein Proteins

After confirming that the Metallothionein (MT) gene had been correctly inserted into the pTYB11 plasmid protein expression was attempted using BL21(DE3) pLysS *E. coli* strain. This strain was chosen originally due to structural and mechanistic features.

This strain of bacteria has key features to facilitate expression of toxic proteins. It contains the T7 RNA Polymerase. This polymerase was derived from a bacteriophage, but has been inserted into various plasmids through transduction techniques. BL21(DE3) pLysS also

contains a T7 lysozyme. This lysozyme has been shown to be critical in controlling T7 RNA Polymerase function. T7 lysozyme binds to T7 RNA Polymerase and inhibits transcription of plasmid mRNA [37]. Incorporating this lysozyme into the BL21 strain allows for transcriptional control and for DNA replication. Furthermore, the *E. coli* cells are able to replicate during their growth phase before being induced.

Another way the BL21(DE3) pLysS strain is able to regulate protein expression is through the expression of Lon and OmpT proteases. The Lon proteases are critical in recognizing and degrading misfolded proteins [38]. The bacterial cell views misfolded proteins as potentially detrimental to cellular health and subsequently eradicates them through the Lon protease mechanism. Therefore, Lon proteases are critical to degradation of proteins expressed within the cellular cytoplasm.

The OmpT proteases are outer-membrane protein proteases. They have a β-barrel domain that crosses the cellular membrane and creates a pore. In the center of the pore is a random loop that contains the enzyme's active site. This protease uses histidine and aspartic acid residues as its active site amino acids [39]. OmpT proteases recognize and cleave proteins with Lys-Lys residues adjacent to each other in the amino acid sequence [39]. Because OmpT proteases are located in the membrane they can degrade proteins attempting to move out or into the cell.

T7 RNA Polymerase is induced using IPTG. When this occurs the polymerase causes all of the bacterial cell's biological processes to switch to creating mRNA and translating plasmid proteins. Once expressed, this polymerase can actually inactivate the host RNA polymerase [40]. Within hours after induction the majority of the cell's cytoplasm will consist of proteins expressed from the plasmid containing T7 RNA Polymerase [40].

MT/Intein Expression Using BL21(DE3) pLysS

When analyzing the SDS gels in Figures 23 and 24 determination of successful expression was based on band appearance at the molecular weight (MW) level of the intein protein, not the MT protein. This is because the small size of the MT protein would run too far down on the gel to measure accurately. Because the expression of MT is done by directly expressing the intein protein connected to MT it is reasonable to directly correlate intein protein expression with MT expression. The reason MT and intein proteins do not stay together in the gel is because β-mercaptethanol is used in the preparation of the proteins for the SDS gel. β-mercaptethanol will break the bond between MT and intein proteins resulting in separate bands on the SDS gel.

The results from the BL21(DE3) pLysS experiments demonstrated no significant level of expression of the MT/intein protein (Figure 21). The SDS gel shows no significant bands at the MW of the intein protein in the induced and non-induced supernatant and pellet lanes. This demonstrated that the BL21(DE3) pLysS cells were not correctly expressing the MT/intein protein.

Even though multiple experiments were conducted utilizing different selected colonies, addition of zinc metals, and adjustment of induction points, there was no evidence that MT was being expressed. It may have been expressed poorly due to Metallothionein's high concentration of cysteine residues, disulfide bonds, and small molecular weight.

Shuffle T7Expression

T7 Shuffle T7 competent cells were selected to test as a better adapted strain for expressing MT.

Shuffle T7 cells are derived from the BL21(DE3) pLysS strain and subsequently the two strains are similar in their components, but with a couple key differences. Shuffle T7 also contains the T7 RNA Polymerase and T7 lysozyme. However, the Shuffle T7 strain contains the Dsbc chaperone protein and lacks the thioredoxin and glutaredoxin genes.

The DsbC protein is critical for the facilitation of folding proteins containing disulfide bonds [41]. The cytoplasm of bacterial and mammalian cells is a reducing environment. Due to the mechanism of such enzymes as thioredoxins and glutaredoxins most disulfide bonds are reduced back to the thiolate state. The DsbC protein acts as a chaperone to oxidize cysteine residues and thus aid in the formation of disulfide bonds. The combination of DsbC chaperone and the lack of reductases allows for increased efficiency of expressing cysteine rich proteins. The formation of disulfide bonds is likely because 20 of the 60 amino acids in MT are cysteines.

Furthermore, the Shuffle strain T7 does not contain the genes for the Lon and OmpT proteases. Because MT could have been misfolded due to the reducing environment and lack of chaperone proteins in the BL21(DE3) pLysS strain, the Lon proteases could have been degrading MT. If so, there could be a significant benefit in using the Shuffle T7 strain where the Lon proteases are not present.

Because OmpT proteases are gatekeepers for extracellular and intracellular protein passage through the membrane, MT could have been degraded by this protease when floating around in the cytoplasm. The OmpT protease cleaves proteins with Lys-Lys residues directly

next to each other. MT has this amino acid sequence at Lys_{30}-Lys_{31}. This implies that OmpT proteases could have been degrading MT through this biochemical mechanism.

MT/Intein Expression Using Shuffle T7 and Western Blot Analysis

The induced band at the MW of the intein protein in Figure 22 provided significant evidence that the intein protein had been successfully expressed using the Shuffle T7 strain. The non-induced supernatant and pellet lanes show no significant levels of protein expression at the MW of the intein protein. This is to be expected because without IPTG protein expression levels are minimal. Furthermore, the empty Shuffle T7 supernatant and pellet lanes indicate no significant levels of protein expression at the MW level of the intein protein.

Even though the SDS gels of the Shuffle T7 expression indicated strong banding at the correct corresponding intein molecular weight level the Li-Cor Western Blot does not suggest that the MT protein was indeed expressed. Shuffle T7 expression samples indicant no significant MT bands. This implies that the MT protein is not present in these samples. The indiscriminate banding present in the mouse liver homogenate lanes indicates faulty antibody bonding and/or that MT was bound to other heavier proteins. Because the MT antibody is over 10 years old it is a definite possibility that the antibody had degraded to the point where recognition of true MT was hindered. The possibility still remains that the intein protein was correctly being expressed, but for some unexplained reason the MT protein was being degraded regardless of any advantages the Shuffle T7 system might have bestowed.

Summary

Using biotechnology techniques the MT gene was excised from pUC57 and inserted into the pTYB11 plasmid. Expression of the MT gene was unsuccessful using the BL21(DE3) pLysS system potentially due to specific biological factors created in this particular strain of E. *coli*. Evidence that expression of the intein protein using the Shuffle T7 system was successful is shown in Figure 22. However, Western Blot analysis of the Shuffle T7 expression provides conflicting evidence as to the ultimate success of expressing MT.

BIBLIOGRAPHY

1. Rosen, D R, T Siddique, D Patterson, D A Figlewicz, P Sapp, A Hentati, D Donaldson, J Goto, J P O'Regan, and H X Deng. 1993. "Mutations in Cu/Zn Superoxide Dismutase Gene Are Associated with Familial Amyotrophic Lateral Sclerosis." *Nature* 362 (6415): 59–62. doi:10.1038/362059a0.
2. Bouldin, Samantha D, Maxwell A Darch, P John Hart, and Caryn E Outten. 2012. "Redox Properties of the Disulfide Bond of Human Cu,Zn Superoxide Dismutase and the Effects of Human Glutaredoxin 1." The Biochemical Journal 446 (1): 59–67. doi:10.1042/BJ20120075.
3. Roberts, Blaine R, John A Tainer, Elizabeth D Getzoff, Dean A Malencik, Sonia R Anderson, Valerie C Bomben, Kathrin R Meyers, P Andrew Karplus, and Joseph S Beckman. 2007. "Structural Characterization of Zinc-Deficient Human Superoxide Dismutase and Implications for ALS." *Journal of Molecular Biology* 373 (4): 877–90. doi:10.1016/j.jmb.2007.07.043.
4. Culotta, Valeria Cizewski, Leo W. J. Klomp, Jeffrey Strain, Ruby Leah B. Casareno, Bernhard Krems, and Jonathan D. Gitlin. 1997. "The Copper Chaperone for Superoxide Dismutase." *Journal of Biological Chemistry* 272 (38): 23469–72. doi:10.1074/jbc.272.38.23469.
5. Maret, Wolfgang. 2011. "Redox Biochemistry of Mammalian Metallothioneins." *Journal of Biological Inorganic Chemistry: JBIC: A Publication of the Society of Biological Inorganic Chemistry* 16 (7): 1079–86. doi:10.1007/s00775-011-0800-0.
6. Forman, Henry J., and Irwin Fridovich. 1973. "On the Stability of Bovine Superoxide Dismutase THE EFFECTS OF METALS." *Journal of Biological Chemistry* 248 (8): 2645–49.
7. Hörnberg, Andreas, Derek T. Logan, Stefan L. Marklund, and Mikael Oliveberg. 2007. "The Coupling between Disulphide Status, Metallation and Dimer Interface Strength in Cu/Zn Superoxide Dismutase." *Journal of Molecular Biology* 365 (2): 333–42. doi:10.1016/j.jmb.2006.09.048.
8. Hart, P. John, Melinda M. Balbirnie, Nancy L. Ogihara, Aram M. Nersissian, Manfred S. Weiss, Joan Selverstone Valentine, and David Eisenberg. 1999. "A Structure-Based Mechanism for Copper−Zinc Superoxide Dismutase†,‡." *Biochemistry* 38 (7): 2167–78. doi:10.1021/bi982284u.
9. Getzoff, E D, J A Tainer, P K Weiner, P A Kollman, J S Richardson, and D C Richardson. 1983. "Electrostatic Recognition between Superoxide and Copper, Zinc Superoxide Dismutase." *Nature* 306 (5940): 287–90.
10. Cleveland, Don W., and Jeffrey D. Rothstein. 2001. "From Charcot to Lou Gehrig: Deciphering Selective Motor Neuron Death in Als." *Nature Reviews Neuroscience* 2 (11): 806–19. doi:10.1038/35097565.
11. Cudkowicz, M. E., D. McKenna-Yasek, P. E. Sapp, W. Chin, B. Geller, D. L. Hayden, D. A. Schoenfeld, B. A. Hosler, H. R. Horvitz, and R. H. Brown. 1997. "Epidemiology of Mutations in Superoxide Dismutase in Amyotrophic Lateal Sclerosis." *Annals of Neurology* 41 (2): 210–21. doi:10.1002/ana.410410212.
12. Crow, J P, Y Z Ye, M Strong, M Kirk, S Barnes, and J S Beckman. 1997. "Superoxide Dismutase Catalyzes Nitration of Tyrosines by Peroxynitrite in the Rod and Head Domains of Neurofilament-L." *Journal of Neurochemistry* 69 (5): 1945–53.

13. Bowling, Allen C., Jorg B. Schulz, Robert H. Brown, and M. Flint Beal. 1993. “Superoxide Dismutase Activity, Oxidative Damage, and Mitochondrial Energy Metabolism in Familial and Sporadic Amyotrophic Lateral Sclerosis.” *Journal of Neurochemistry* 61 (6): 2322–25. doi:10.1111/j.1471-4159.1993.tb07478.x.
14. Crow, John P., Jacinda B. Sampson, Yingxin Zhuang, John A. Thompson, and Joseph S. Beckman. 1997. “Decreased Zinc Affinity of Amyotrophic Lateral Sclerosis-Associated Superoxide Dismutase Mutants Leads to Enhanced Catalysis of Tyrosine Nitration by Peroxynitrite.” *Journal of Neurochemistry* 69 (5): 1936–44. doi:10.1046/j.1471-4159.1997.69051936.x.
15. Estévez, Alvaro G., John P. Crow, Jacinda B. Sampson, Christopher Reiter, Yingxin Zhuang, Gloria J. Richardson, Margaret M. Tarpey, Luis Barbeito, and Joseph S. Beckman. 1999. “Induction of Nitric Oxide -- Dependent Apoptosis in Motor Neurons by Zinc-Deficient Superoxide Dismutase.” *Science* 286 (5449): 2498–2500. doi:10.1126/science.286.5449.2498.
16. Beckman, J S, M Carson, C D Smith, and W H Koppenol. 1993. “ALS, SOD and Peroxynitrite.” *Nature* 364 (6438): 584. doi:10.1038/364584a0.
17. Beckman, Joseph S. 1996. “Oxidative Damage and Tyrosine Nitration from Peroxynitrite.” *Chemical Research in Toxicology* 9 (5): 836–44. doi:10.1021/tx9501445.
18. Franco, Maria Clara, Yaozu Ye, Christian A. Refakis, Jessica L. Feldman, Audrey L. Stokes, Manuela Basso, Raquel M. Melero Fernández de Mera, et al. 2013. “Nitration of Hsp90 Induces Cell Death.” *Proceedings of the National Academy of Sciences* 110 (12): E1102–E1111. doi:10.1073/pnas.1215177110.
19. Raoul, Cedric, Christopher E. Henderson, and Brigitte Pettmann. 1999. “Programmed Cell Death of Embryonic Motoneurons Triggered through the FAS Death Receptor.” *The Journal of Cell Biology* 147 (5): 1049–62.
20. Jiang, Xuejun, and Xiaodong Wang. 2004. “Cytochrome C-Mediated Apoptosis.” *Annual Review of Biochemistry* 73: 87–106. doi:10.1146/annurev.biochem.73.011303.073706.
21. Raoul, Cédric, Alvaro G. Estévez, Hiroshi Nishimune, Don W. Cleveland, Odile deLapeyrière, Christopher E. Henderson, Georg Haase, and Brigitte Pettmann. 2002. “Motoneuron Death Triggered by a Specific Pathway Downstream of Fas: Potentiation by ALS-Linked SOD1 Mutations.” *Neuron* 35 (6): 1067–83. doi:10.1016/S0896-6273(02)00905-4.
22. Bjartmar, C, J. R Wujek, and B. D Trapp. 2003. “Axonal Loss in the Pathology of MS: Consequences for Understanding the Progressive Phase of the Disease.” *Journal of the Neurological Sciences* 206 (2): 165–71. doi:10.1016/S0022-510X(02)00069-2.
23. Saxena, Smita, and Pico Caroni. 2007. “Mechanisms of Axon Degeneration: From Development to Disease.” *Progress in Neurobiology* 83 (3): 174–91. doi:10.1016/j.pneurobio.2007.07.007.
24. Gould, Thomas W., Robert R. Buss, Sharon Vinsant, David Prevette, Woong Sun, C. Michael Knudson, Carol E. Milligan, and Ronald W. Oppenheim. 2006. “Complete Dissociation of Motor Neuron Death from Motor Dysfunction by Bax Deletion in a Mouse Model of ALS.” *The Journal of Neuroscience* 26 (34): 8774–86. doi:10.1523/JNEUROSCI.2315-06.2006.
25. Loeb, Gerald. “The Motor Unit and Muscle Action.” Textbook, 675–94.

26. Burke, R. E., D. N. Levine, P. Tsairis, and F. E. Zajac. 1973. “Physiological Types and Histochemical Profiles in Motor Units of the Cat Gastrocnemius.” *The Journal of Physiology* 234 (3): 723–748.3.
27. Vinsant, Sharon, Carol Mansfield, Ramon Jimenez-Moreno, Victoria Del Gaizo Moore, Masaaki Yoshikawa, Thomas G Hampton, David Prevette, James Caress, Ronald W Oppenheim, and Carol Milligan. 2013. “Characterization of Early Pathogenesis in the SOD1(G93A) Mouse Model of ALS: Part II, Results and Discussion.” *Brain and Behavior* 3 (4): 431–57. doi:10.1002/brb3.142.
28. Margoshes, Marvin, and Bert L. Vallee. 1957. “A CADMIUM PROTEIN FROM EQUINE KIDNEY CORTEX.” *Journal of the American Chemical Society* 79 (17): 4813–14. doi:10.1021/ja01574a064.
29. KAGI, J H, and B L VALEE. 1960. “Metallothionein: A Cadmium- and Zinc-Containing Protein from Equine Renal Cortex.” *The Journal of Biological Chemistry* 235 (December): 3460–65.
30. Maret, Wolfgang, and Bert L. Vallee. 1998. “Thiolate Ligands in Metallothionein Confer Redox Activity on Zinc Clusters.” *Proceedings of the National Academy of Sciences* 95 (7): 3478–82.
31. Thirumoorthy, N., A. Shyam Sunder, KT Manisenthil Kumar, M. Senthil Kumar, G. N. K. Ganesh, and Malay Chatterjee. 2011. “A Review of Metallothionein Isoforms and Their Role in Pathophysiology.” *World Journal of Surgical Oncology* 9 (1): 54. doi:10.1186/1477-7819-9-54.
32. West, Adrian K., Juan Hidalgo, Donnie Eddins, Edward D. Levin, and Michael Aschner. 2008. “Metallothionein in the Central Nervous System: Roles in Protection, Regeneration and Cognition.” *Neurotoxicology* 29 (3): 488–502. doi:10.1016/j.neuro.2007.12.006.
33. Tokuda, Eiichi, Shin-Ichi Ono, Kumiko Ishige, Akira Naganuma, Yoshihisa Ito, and Takashi Suzuki. 2007. “Metallothionein Proteins Expression, Copper and Zinc Concentrations, and Lipid Peroxidation Level in a Rodent Model for Amyotrophic Lateral Sclerosis.” *Toxicology* 229 (1-2): 33–41. doi:10.1016/j.tox.2006.09.011.
34. Chan, Jayna, Zuyun Huang, Maureen E Merrifield, Maria T Salgado, and Martin J Stillman. 2002. “Studies of Metal Binding Reactions in Metallothioneins by Spectroscopic, Molecular Biology, and Molecular Modeling Techniques.” *Coordination Chemistry Reviews* 233–234 (November): 319–39. doi:10.1016/S0010-8545(02)00176-5.
35. Andreini, Claudia, Lucia Banci, Ivano Bertini, and Antonio Rosato. 2006. “Counting the Zinc-Proteins Encoded in the Human Genome.” *Journal of Proteome Research* 5 (1): 196–201. doi:10.1021/pr050361j.
36. Hong, S, M Toyama, W Maret, and Y Murooka. 2001. “High Yield Expression and Single Step Purification of Human Thionein/metallothionein.” *Protein Expression and Purification* 21 (1): 243–50. doi:10.1006/prep.2000.1372.
37. Cheng, X, X Zhang, J W Pflugrath, and F W Studier. 1994. “The Structure of Bacteriophage T7 Lysozyme, a Zinc Amidase and an Inhibitor of T7 RNA Polymerase.” *Proceedings of the National Academy of Sciences of the United States of America* 91 (9): 4034–38.
38. Breidenstein, Elena B M, Laure Janot, Janine Strehmel, Lucia Fernandez, Patrick K Taylor, Irena Kukavica-Ibrulj, Shaan L Gellatly, Roger C Levesque, Joerg Overhage, and Robert E W Hancock. 2012. “The Lon Protease Is Essential for Full Virulence in Pseudomonas Aeruginosa.” *PloS One* 7 (11): e49123. doi:10.1371/journal.pone.0049123.

39. Baaden, Marc, and Mark S P Sansom. 2004. “OmpT: Molecular Dynamics Simulations of an Outer Membrane Enzyme.” *Biophysical Journal* 87 (5): 2942–53. doi:10.1529/biophysj.104.046987.
40. Davanloo, P, A H Rosenberg, J J Dunn, and F W Studier. 1984. “Cloning and Expression of the Gene for Bacteriophage T7 RNA Polymerase.” *Proceedings of the National Academy of Sciences of the United States of America* 81 (7): 2035–39.
41. Chen, J, J L Song, S Zhang, Y Wang, D F Cui, and C C Wang. 1999. “Chaperone Activity of DsbC.” *The Journal of Biological Chemistry* 274 (28): 19601–5.